Three-dimensional phononic crystal with ultra-wide bandgap for ultrasonics applications

Eg-MRS 2021

Vincent Laude

Institut FEMTO-ST
Centre National de la Recherche Scientifique (CNRS),
Univ. Bourgogne Franche-Comté, Besançon, France

July 2021

Contents

Artificial crystals

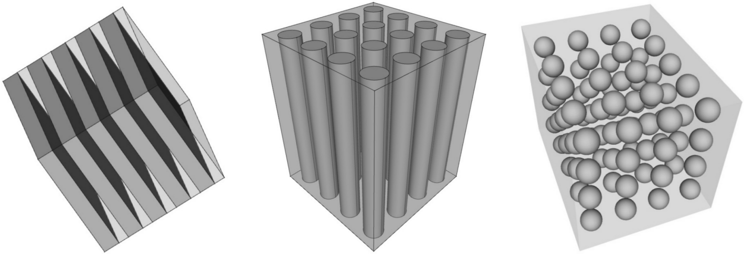

Figure: **Artificial crystals for waves with 1D, 2D, or 3D periodicity**

- Sonic crystal: matrix is a fluid (e.g., water or air)
- Phononic crystal: matrix is a solid (e.g., steel, silicon, quartz...) [1]
- Inclusions can be void, solid, or fluid

Bloch theorem

Helmholtz equation with periodic coefficients: $-\nabla \cdot (c(\boldsymbol{r})\nabla u(\boldsymbol{r})) = \omega^2 u(\boldsymbol{r})$

Theorem (Bloch)

The eigenmodes of the periodic Helmholtz equation are Bloch waves of the form

$$u(\boldsymbol{r}) = \exp(-\imath \boldsymbol{k} \cdot \boldsymbol{r})\tilde{u}(\boldsymbol{r})$$

where $\tilde{u}(\boldsymbol{r})$ is a periodic function with the same periodicity as the crystal and $\boldsymbol{k}$ is the Bloch wave vector.

(Classical) band structure: solve for $\omega(k)$ with $\boldsymbol{k}$ inside the first Brillouin zone

Sonic crystal of cylindrical steel rods in water: band structure

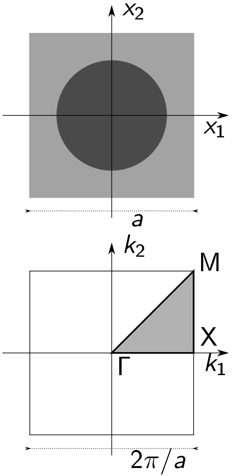

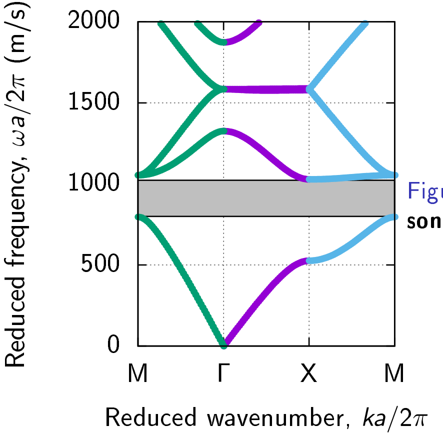

Figure: **2D square-lattice sonic crystal**. $d/a = 0.83$

A square-lattice phononic crystal of steel rods in water: transmission

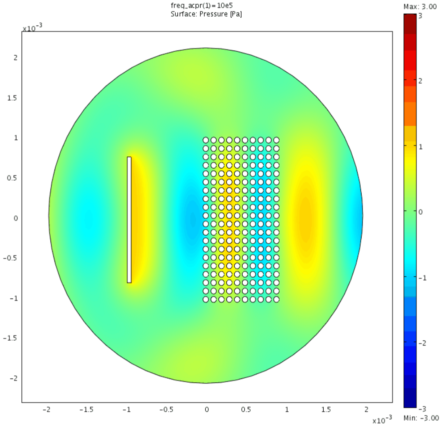

- Pitch: 100 μm
- Diameter: 70 μm
- Complete band gap: 8-9 MHz
- Plane source emits 1 Pa

FEM meshes for 3D sonic crystals

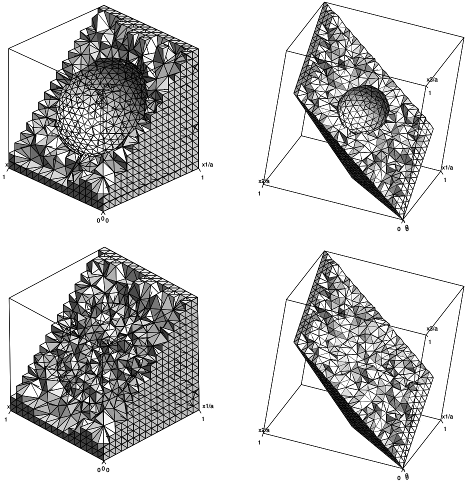

Figure: 3D meshes for simple cubic (SC, left) and face centered cubic (FCC, right) lattice sonic crystals.

Air bubbles in water

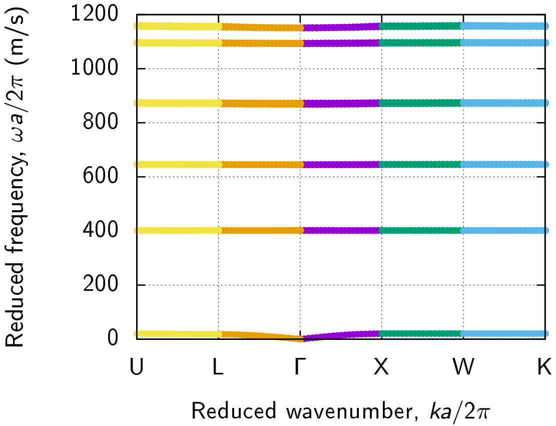

Figure: **Band structure of fcc lattice sonic crystal of air bubbles in water.** $d/a = 0.3628$.

Examples of phononic crystals

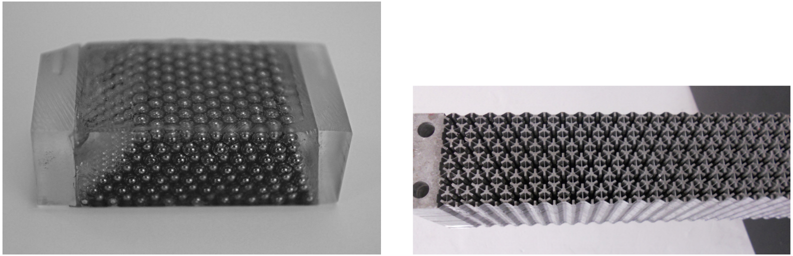

(a) (b)

Figure: **Examples of phononic crystals.** (a) 3D phononic crystal of steel spheres in an epoxy matrix arranged according to a FCC lattice [2]. (b) 2D phononic crystal of holes in aluminum [3].

Elastodynamic equations

- Dynamic equation

$$T_{ij,j} + f_i = \rho \frac{\partial^2 u_i}{\partial t^2}$$

- u is the displacement vector, T_{ij} is the stress tensor
- f_i are body forces (often, sources)
- Constitutive equation of elasticity (Hooke's law)

$$T_{ij} = c_{ijkl} S_{kl}$$

with c_{ijkl} the elastic tensor and $S_{ij} = \frac{1}{2}(u_{i,j} + u_{j,i})$ the strain tensor.
- Contracted notation: $I = (ij)$ for any pair of symmetric indices. $I = 1 \cdots 6$. $T_I = c_{IJ} S_J$.
- In phononic crystals, the material tensors are discontinuous functions of position.

Weak form of the elastodynamic equation, boundary conditions

- Consider test functions v that are defined on the same finite element space as the displacement vector u. Projection on the test functions results in

$$-\int_\Omega dr\, \mathrm{v}^* \cdot (\nabla \cdot T) + \int_\Omega dr\, \mathrm{v}^* \cdot \rho \frac{\partial^2 \mathrm{u}}{\partial t^2} = \int_\Omega dr\, \mathrm{v}^* \cdot \mathrm{f}$$

- Apply the divergence theorem and insert Hooke's law to get

$$\int_\Omega dr\, S(\mathrm{v})_I^* c_{IJ} S(\mathrm{u})_J - \int_\sigma ds\, \mathrm{v}^* \cdot T_n + \int_\Omega dr\, \mathrm{v}^* \cdot \rho \frac{\partial^2 \mathrm{u}}{\partial t^2} = \int_\Omega dr\, \mathrm{v}^* \cdot \mathrm{f}$$

  $T_n = T_{ij} n_j$ is the normal traction.
- External boundary conditions – free: $T_n = 0$; Dirichlet: $u_i = u_{0i}$
- Continuity between elements of displacements and normal tractions.

FEM for a unit-cell: the band structure of phononic crystals

Apply periodic boundary conditions and consider Bloch waves as $u_i(t, \boldsymbol{x}) = \tilde{u}_i(\boldsymbol{x}) \exp(\imath(\omega t - \boldsymbol{k} \cdot \boldsymbol{x}))$

$$\int_\Omega dr\ S(\mathrm{v})_I^* c_{IJ} S(\mathrm{u})_J = \omega^2 \int_\Omega dr\ \mathrm{v}^* \cdot \rho \mathrm{u}$$

where the strains should be understood as

$$S_1(\mathrm{u}) = \frac{\partial \tilde{u}_1}{\partial x_1} - \imath k_1 \tilde{u}_1,$$

$$S_2(\mathrm{u}) = \frac{\partial \tilde{u}_2}{\partial x_2} - \imath k_2 \tilde{u}_2,$$

$$S_3(\mathrm{u}) = \frac{\partial \tilde{u}_3}{\partial x_3} - \imath k_3 \tilde{u}_3,$$

$$S_4(\mathrm{u}) = \frac{\partial \tilde{u}_3}{\partial x_2} + \frac{\partial \tilde{u}_2}{\partial x_3} - \imath(k_3 \tilde{u}_2 + k_2 \tilde{u}_3),$$

$$S_5(\mathrm{u}) = \frac{\partial \tilde{u}_3}{\partial x_1} + \frac{\partial \tilde{u}_1}{\partial x_3} - \imath(k_3 \tilde{u}_1 + k_1 \tilde{u}_3),$$

$$S_6(\mathrm{u}) = \frac{\partial \tilde{u}_2}{\partial x_1} + \frac{\partial \tilde{u}_1}{\partial x_2} - \imath(k_2 \tilde{u}_1 + k_1 \tilde{u}_2).$$

3D FCC-lattice phononic crystal of steel spheres in epoxy

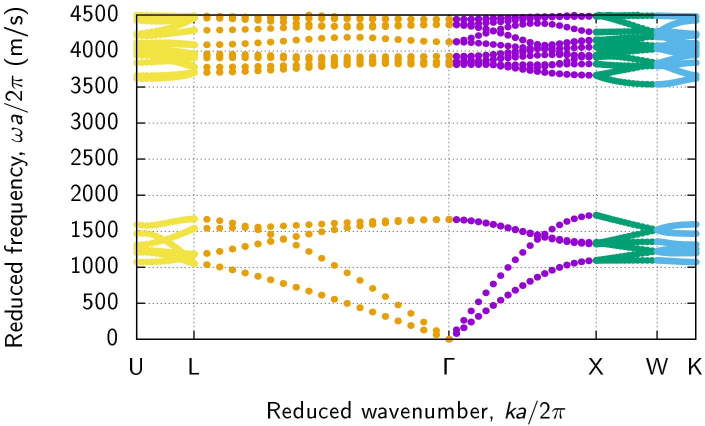

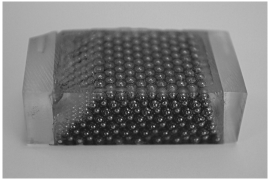

Figure: The filling fraction is $F = 0.74$ ($d/a = 0.707$) [2].

Steel spheres in epoxy, 3D close-packed FCC

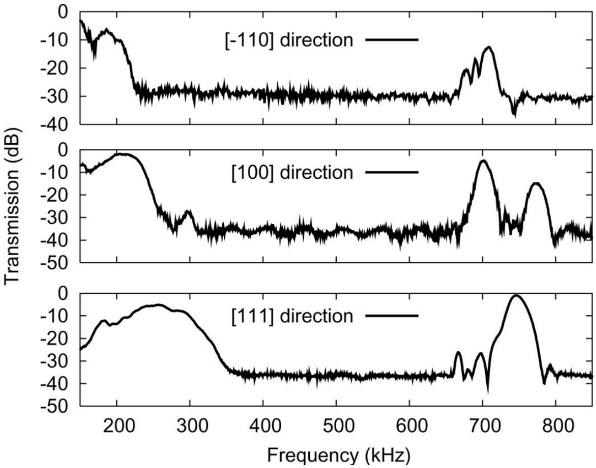

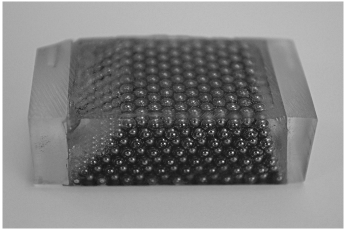

Figure: Experimental transmission power spectra along (a) the $[\bar{1}10]$, (b) the [100], and (c) the [111] directions of a 4-period PC [2].

[2] Khelif et al, IEEE TUFFC 2010

Tragazikis et al, J. Phys. D 2019

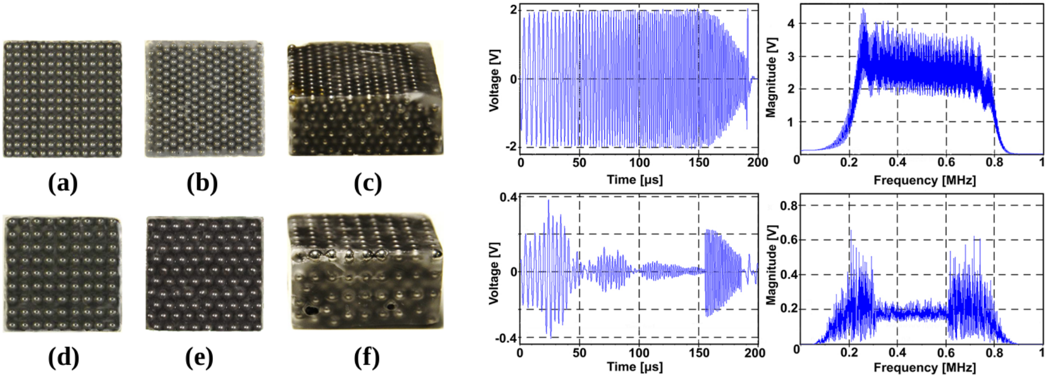

Crystals of steel balls (close-packed spheres) in paraffin, hcp [4]

D'Alessandro et al, Appl. Phys. Lett. 2016

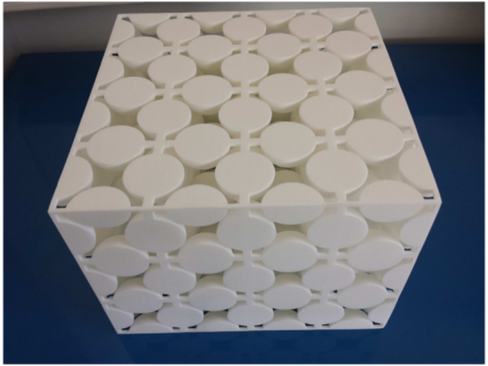

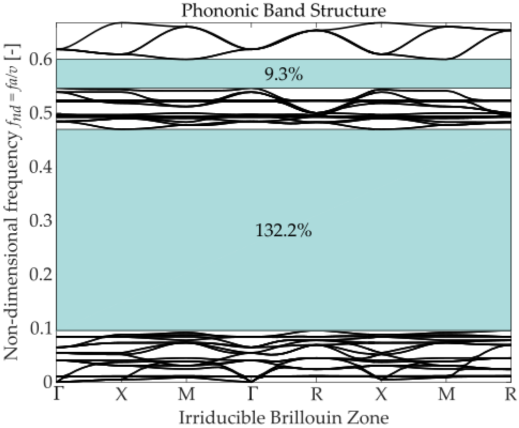

Perovskite-cubic crystal [5], 3D printed (SLS, selective laser sintering), around 11 kHz

Warmuth et al, Sci. Rep. 2017

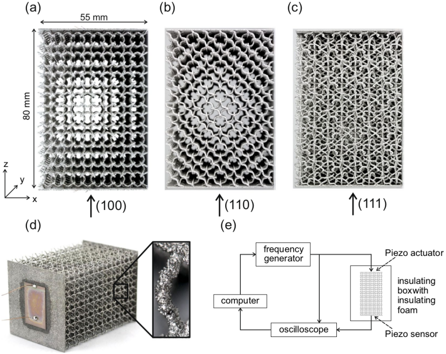

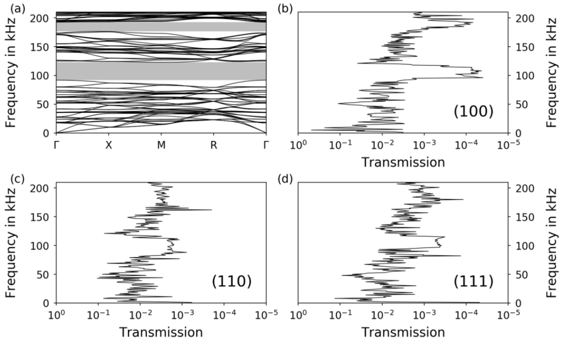

Simple cubic [8], 3D printed (SBEM, selective electron beam melting), around 90 kHz

Lucklum et al, Appl. Phys. Lett. 2018

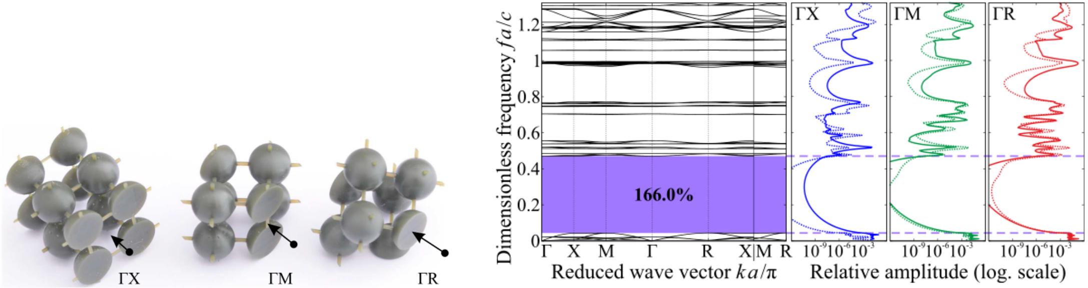

Simple cubic [6], 3D printed (SLA, stereolithography apparatus), around 55 kHz

McGee et al, Additive Manufacturing 2019

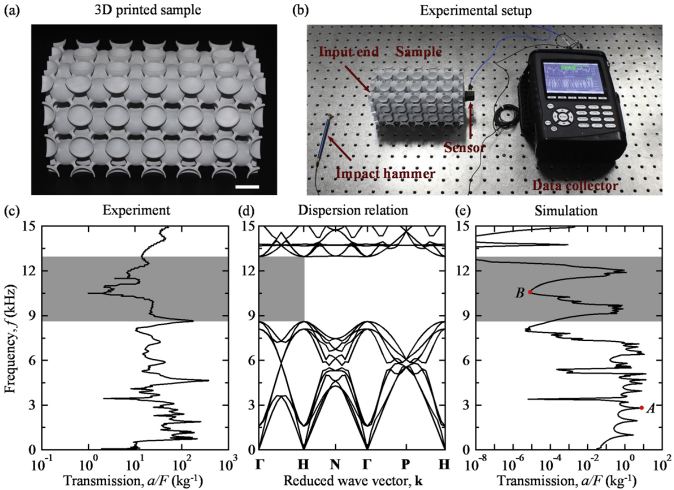

Body-centered cubic [7], 3D printed (SLS, selective laser sintering), around 11 kHz

State of the art for band gap width

How do we reach ultrasonic frequencies (> 1 MHz)?

A smaller lattice constant is required

Table: 3D phononic crystals. pc: perovskite-cubic; fcc: face-centered cubic; hcp: hexagonal compact; sc: simple cubic; bcc: body-centered cubic; SLS: selective laser sintering; SLA: stereolithography apparatus; SBEM: Selective Electron Beam Melting.

Symmetry	Fabrication	ω_g	$\Delta\omega/\omega_g$
pc [this work]	3D printing (TPL)	4 MHz	170%
fcc [2]	steel balls and epoxy	500 kHz	60%
hcp [4]	steel balls and paraffin	635 kHz	72%
pc [5]	3D printing (SLS)	11.36 kHz	132%
sc [6]	3D printing (SLA)	55 kHz	166%
bcc [7]	3D printing (SLS)	11.3 kHz	48%
sc [8]	3D printing (SBEM)	90 kHz	22%

Two-photon lithography in photopolymer (Nanoscribe)

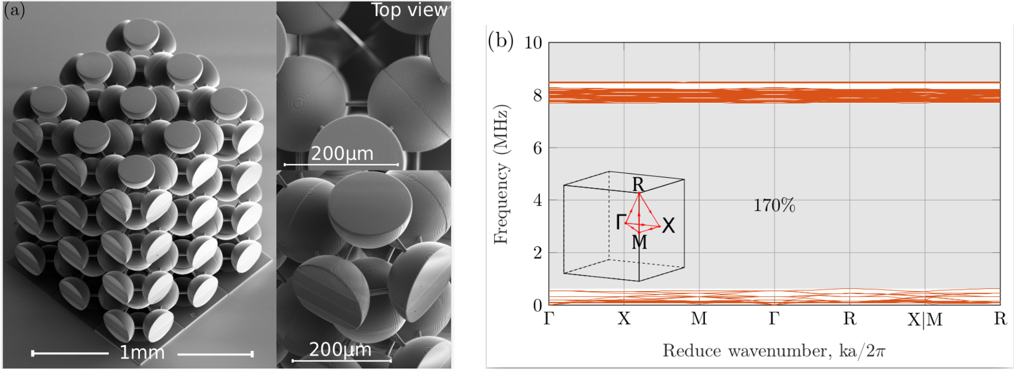

Perovskite-cubic crystal, large spheres (masses) connected by thin struts (diameter: 3 µm)
Three-dimensional phononic crystal with ultra-wide bandgap at megahertz frequencies, Iglesias Martínez et al, Appl. Phys. Lett. **118** 063507 (2021)

Determination of Young's modulus

Method

3D print rectangular-section beams, observe the fundamental vibration mode, compare with beam theory to fit E, Young's modulus. Poisson's ratio is determined from compression experiments. Alternative: we also use Brillouin light scattering.

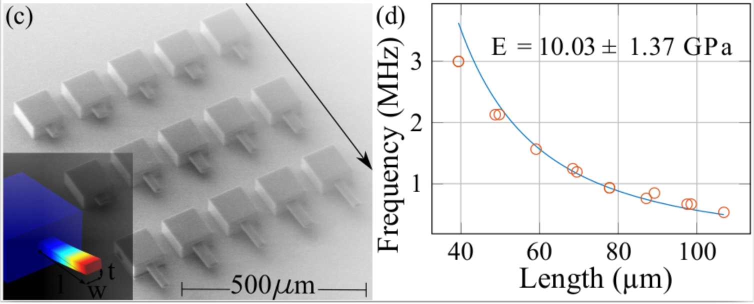

Vibration metrology: Polytec microsystem analyzer

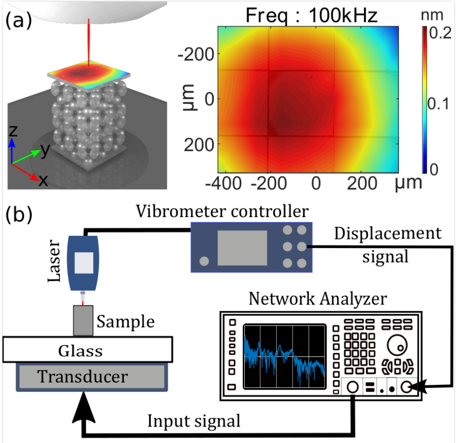

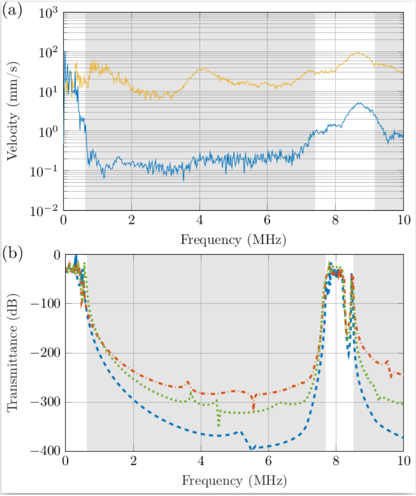

Some possible concerns about operation and measurements

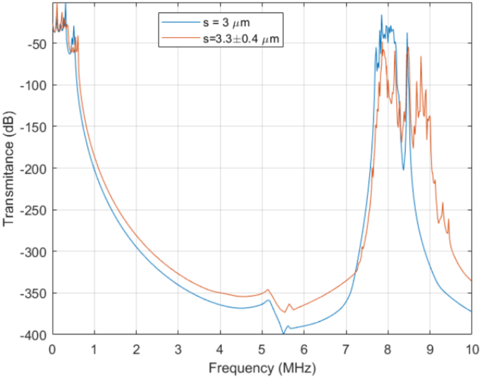

Errors on strut diameter?

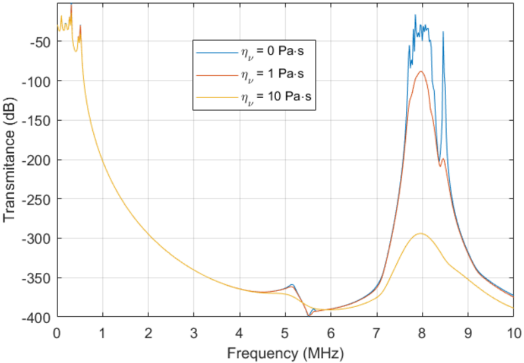

Influence of viscoelastic loss?

Nonlinear isotropy for energy absorption

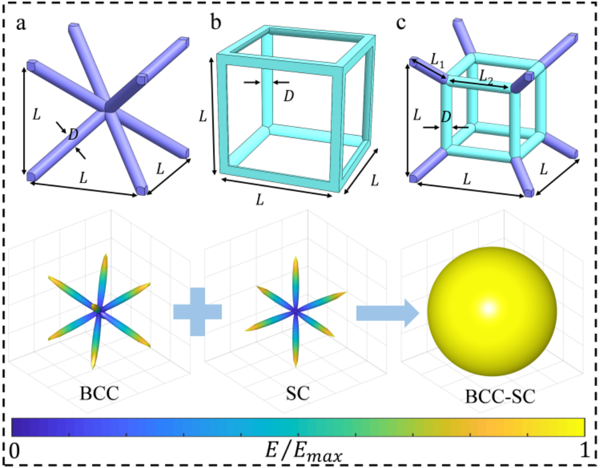

- The BCC lattice is extremely anisotropic, strong along diagonals, weak along cubic axes
- The SC lattice is also extremely anisotropic, weak along diagonals, strong along cubic axes
- The SC-BCC lattice is a continuous morphing between them and becomes isotropic at some point

Nonlinear isotropy for energy absorption

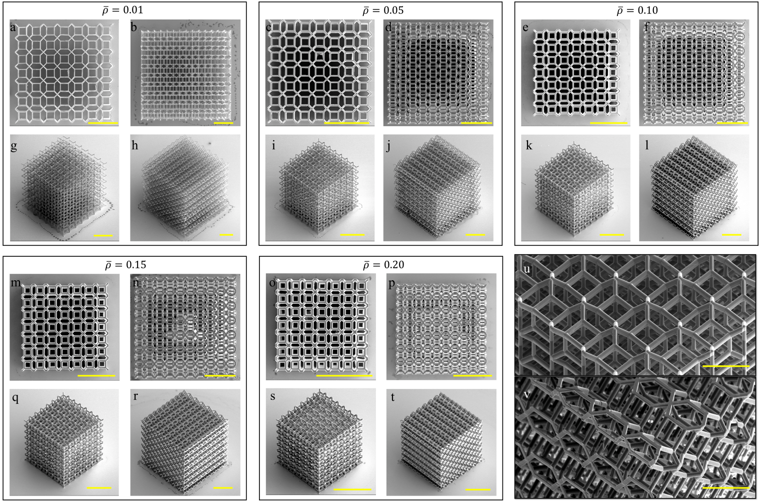

Samples fabricated using two-photon lithography.
Scale bar: 100 μm.

Nonlinear isotropy for energy absorption

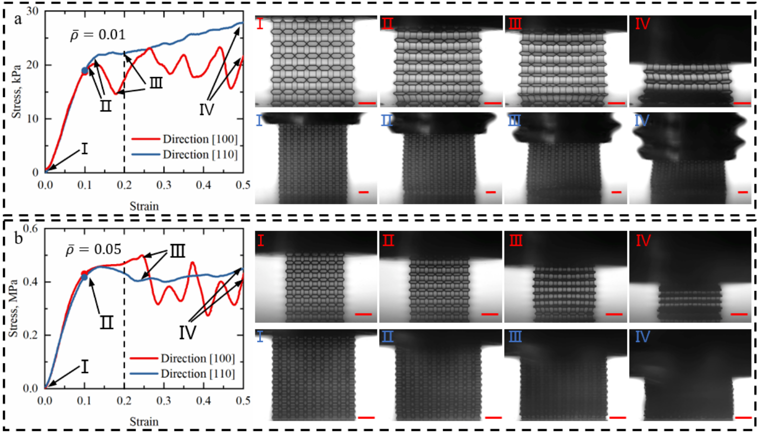

Compression tests. Strains are measured by digital image correlation. Scale bar: 100 μm.

Zero Poisson's ratio: an artificial isotropic cork material?

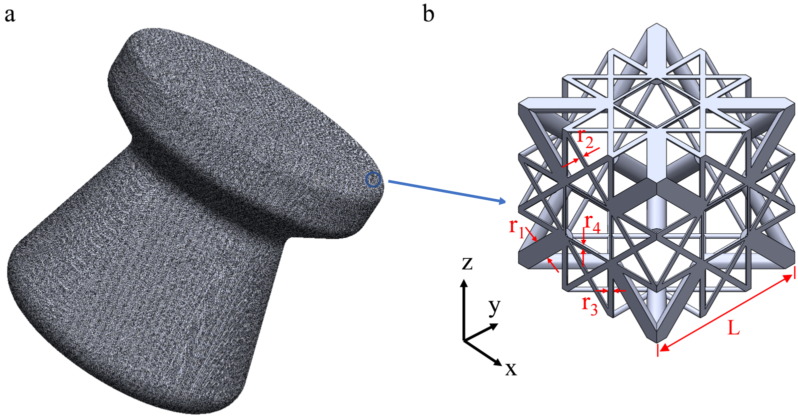

Zero Poisson's ratio: Two-photon lithography samples

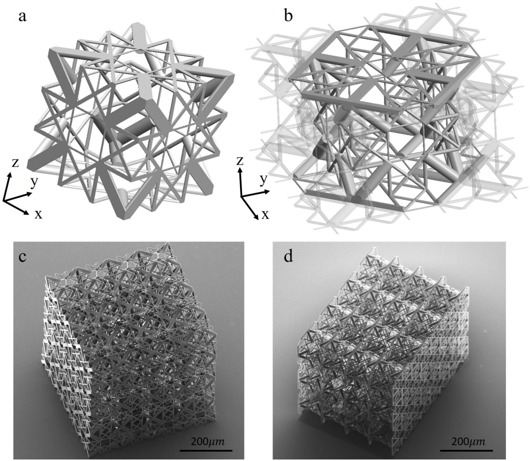

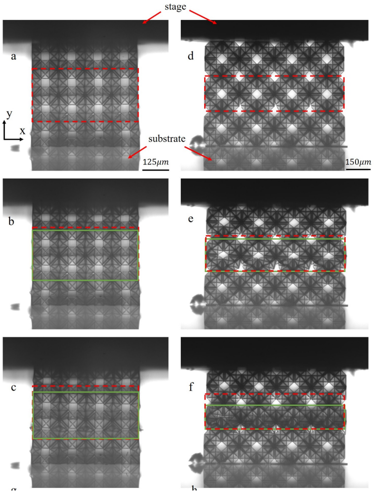

Conclusion and outlook

- Additive manufacturing techniques allow fabrication of 3D phononic crystals with complex unit-cells
- Beyond close-packed assembly, the phononic band gap can be optimized. The maximum band gap width would be 200%
- Ultrasonic frequencies (> 1 MHz) require sub-micron resolution: two-photon lithography is suitable
- 3D phononic crystals meet mechanical metamaterials at that scale

References I

[1] M. S. Kushwaha, P. Halevi, L. Dobrzynski, and B. Djafari-Rouhani.
Acoustic band structure of periodic elastic composites.
Phys. Rev. Lett., 71(13):2022–2025, 1993.

[2] Abdelkrim Khelif, Fu-Li Hsiao, Abdelkrim Choujaa, Sarah Benchabane, and Vincent Laude.
Octave omnidirectional band gap in a three-dimensional phononic crystal.
IEEE Trans. Ultrason., Ferroelec., Freq. Control, 57(7):1621, 2010.

[3] A.-C. Hladky-Hennion, J. O. Vasseur, G. Haw, C. Croënne, L. Haumesser, and A. N. Norris.
Negative refraction of acoustic waves using a foam-like metallic structure.
Appl. Phys. Lett., 102(14):144103, 2013.

[4] I. K. Tragazikis, D. A. Exarchos, P. T. Dalla, K. Dassios, T. E. Matikas, and I. E. Psarobas.
Elastodynamic response of three-dimensional phononic crystals using laser Doppler vibrometry.
J. Phys. D: Appl. Phys., 52(28):285305, 2019.

[5] L. D'Alessandro, E. Belloni, R. Ardito, A. Corigliano, and F. Braghin.
Modeling and experimental verification of an ultra-wide bandgap in 3D phononic crystal.
Appl. Phys. Lett., 109(22):221907, 2016.

[6] Frieder Lucklum and Michael J. Vellekoop.
Bandgap engineering of three-dimensional phononic crystals in a simple cubic lattice.
Appl. Phys. Lett., 113(20):201902, 2018.

[7] Olivia McGee, Huan Jiang, Feng Qian, Zian Jia, Lifeng Wang, Han Meng, Dimitrios Chronopoulos, Yanyu Chen, and Lei Zuo.
3D printed architected hollow sphere foams with low-frequency phononic band gaps.
Additive Manufacturing, 30:100842, 2019.

References II

[8] Franziska Warmuth, Maximilian Wormser, and Carolin Körner.
Single phase 3D phononic band gap material.
Scientific Reports, 7(1):3843, 2017.